American Mineralogist, Volume 68, pages 754–758, 1983

Interlayering and interlayer slip in biotite as seen by HRTEM

JUAN OLIVES BAÑOS, MARC AMOURIC

Centre de Recherche sur les Mécanismes de la Croissance Cristalline (CRMC2-CNRS), Campus de Luminy, case 913, 13288 Marseille cedex 09, France

CHANTAL DE FOUQUET

Ecole Nationale Supérieure des Mines de Paris, Centre de Géostatistique 33, rue Saint-Honoré, 77300 Fontainebleau, France

AND ALAIN BARONNET

Centre de Recherche sur les Mécanismes de la Croissance Cristalline (CRMC2-CNRS), Campus de Luminy, case 913, 13288 Marseille cedex 09, France

Abstract

Interlayering, slip, and cleavage phenomena have been observed using high-resolution transmission electron microscopy in tectonically deformed biotite. The unit mica layers and the positions of the interlayer cations can be imaged with this technique. From the observations, we conclude first that slip and cleavage occur in the interlayer level of the structure. The biotite shows partial interlayers of brucite-like sheets, which form, with the adjacent talc-like layers of the mica, single chlorite layers interstratified in the mica structure. From structural and physical considerations, brucite interlayering is interpreted here as a "brucitization" of an interlayer level of the mica where partial slip or cleavage has previously occurred. It is an example of a chemical process at the atomic scale (local chloritization of the mica) favored by deformation microstructures.

Introduction

Transmission electron microscopy (TEM) has revealed recently the intercalation of isolated 14Å-thick chlorite or smectite layers in sericite and biotite (McKee and Buseck, 1978; Page and Wenk, 1979; Iijima and Zhu, 1982). Veblen and Buseck (1980, 1981) have observed, in high-resolution images, the partial interlayering of a brucite-like sheet (~5Å thick) in talc (9.3Å spacing). In the present study, high-resolution TEM (HRTEM) is used to describe partial interstratification of a brucite-like sheet in the mica structure. Showing that slip in micas occurs in the interlayer level, we suggest that brucite interlayering forms here by "brucitization" of an interlayer level of the mica occurring after an interlayer partial slip or a cleavage.

The micas studied are biotites belonging to the Bormes gneisses (Maures massif, Var, France). The origin of this formation is interpreted as an intrusive granite (Tempier *et al.*, 1980). The whole massif has been affected by a Barrovian syntectonic progressive metamorphism of caledonian and/or hercynian age. Bormes gneisses were in the mesozone. The tectonic history is characterized by generations of early tight folds and later open and chevron-type folds (for details on the tectonics in the epizonal terranes, see Olives and Fonteilles, 1980). Our gneiss sample has been affected by centimetric chevron folds (with axial plane dipping northeastward) and the micas have been deformed (bent and kinked) by these folds.

Technique

The HRTEM images which give most structural information are obtained with micas having their basal plane parallel to the electron beam (see the next section). The basal plane of micas being statistically parallel to the gneiss foliation, we have started with conventional petrographic thin sections perpendicular to the axis (on the foliation) of the chevron folds. The sections were mounted with Lakeside cement. Copper grids or rings 2–3 mm in diameter were glued to the rock slice with Araldite on mica zones selected with the optical microscope. The rock was then removed from the slide glass by heating until the Lakeside became fluid. The samples were thinned in an argon ion miller at low beam incidence angles. We have used a JEM 100C microscope operating at 100 kV with an objective lens of spherical aberration coefficient 1.7 mm and an objective aperture of 35 μm.

0003–004X/83/0708–0754$02.00

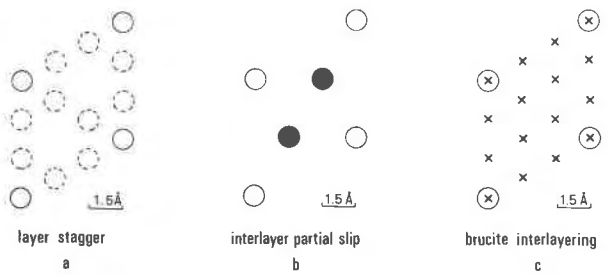

Fig. 1. Centers of hexagons of two tetrahedral sheets T_1 and T_2 in different structural arrangements (projection onto the basal plane): white circles—centers of hexagons of T_1; dashed circles—possible positions for centers of hexagons of T_2, if T_1 and T_2 are joined by an octahedral sheet O and form a talc layer T_1–O–T_2; black circles—possible positions for centers of hexagons of T_2, if T_1 and T_2 are separated by an interlayer level with partial slip in this level; crosses—possible positions for centers of hexagons of T_2, if T_1 and T_2 are separated by a brucite sheet.

Images with optimum defocus were selected from image series taken at successive experimental defocus values from −800 to −1200Å.

Mica structure imaging

The mica structure consists of talc-like layers (T–O–T layers where T are tetrahedral sheets and O an octahedral sheet) alternating with planes of potassium ions (interlayer level). The distance between two consecutive interlayer levels is approximately 10Å. Tetrahedral sheets are formed by hexagons of tetrahedra, each tetrahedron belonging to three hexagons and occupying a central position relative to them: centers of tetrahedra are represented by black circles in Figure 1b and the centers of hexagons by white circles (for details on mica structure, see Smith and Yoder, 1956). The interlayer cations project onto the centers of hexagons. The centers of hexagons of two tetrahedral sheets T_1 and T_2 of a talc layer T_1–O–T_2 (or the corresponding interlayer cations) are shifted relative to one another by a "layer stagger" which is the vector joining a white circle to a neighboring dashed circle in Figure 1a.

Bright-field HRTEM images of micas in which the layers are parallel to the electron beam direction generally show dark bands separated by thin bright fringes of 10Å periodicity (see Figs. 2–4). Great care is needed in the interpretation of image contrast, which is affected by dynamical diffraction and may have no direct structural interpretation (Amouric *et al.*, 1981). In our images, obtained at an optimum defocus, we have frequently noted partial microcleavages. The microcleavages always terminate in a bright fringe (Fig. 2). Deville and Goldsztaub (1969) have shown that cleavage occurs in the interlayer level. Thus, we conclude that the thin bright fringes correspond to interlayer levels. In this case, the image contrast (bright fringes) and structure (low density of atoms in the interlayer level) are concordant.

If the mica is oriented in such a way that a close-packed row of interlayer cations (for example, the vertical direction in Fig. 1) is parallel to the electron beam, and under certain microscope experimental conditions, the bright fringes are discontinuous and consist of bright spots periodically spaced 4.5Å apart (Fig. 5). The most reasonable structural interpretation of these spots is that they correspond to the "channels" (low electron density) situated between two consecutive close-packed rows of interlayer cations (Iijima and Buseck, 1978; Amouric *et al.*, 1978). The shift between the spots on two successive levels should therefore represent the layer stagger projected onto the image plane which is 0 or ±1.5Å (see Fig. 1a and suppose the image plane to be horizontal), and this has been confirmed in HRTEM images (authors referred to above). We shall use here the "channel interpretation" of spots, as it leads us to a consistent understanding of brucite interlayering.

Interlayer slip

Bending and kinking of our micas have been produced by intracrystalline basal slip. In general, since the first observations of Silk and Barnes (1961), crystal defects such as dislocations or planar defects have been known to lie on basal planes. However, their exact localization—at the scale of interatomic distances—remains undetermined. Two regions, the interlayer level and the octahedral sheet, have been suggested (Caslavsky and Vedam, 1970; Sitarek and Becherer, 1974; Bell and Wilson, 1977). Although much information can be obtained with conventional TEM (see Bell and Wilson, 1981), only structure imaging using HRTEM is able to solve such questions. Figure 2 shows a microcleavage of unsymmetric shape which has been produced by basal slip. This image shows clearly that slip has occurred in the same atomic plane as cleavage, that is to say in the interlayer level. This observation and the knowledge of Burgers vectors of partial defects (by the authors referred to immediately above) lead to the interpretation of partial basal slip as a definite displacement between the two tetrahedral sheets T_1 and T_2 separated by the interlayer level (Caslavsky and Vedam, 1970). The shift is one of the vectors joining a

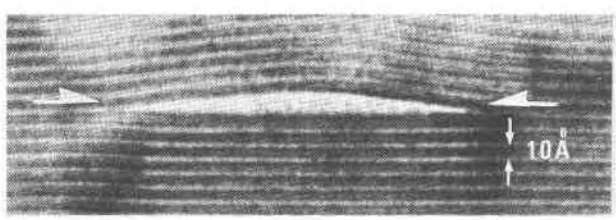

Fig. 2. Limited microcleavage in mica produced by basal slip in the interlayer level.

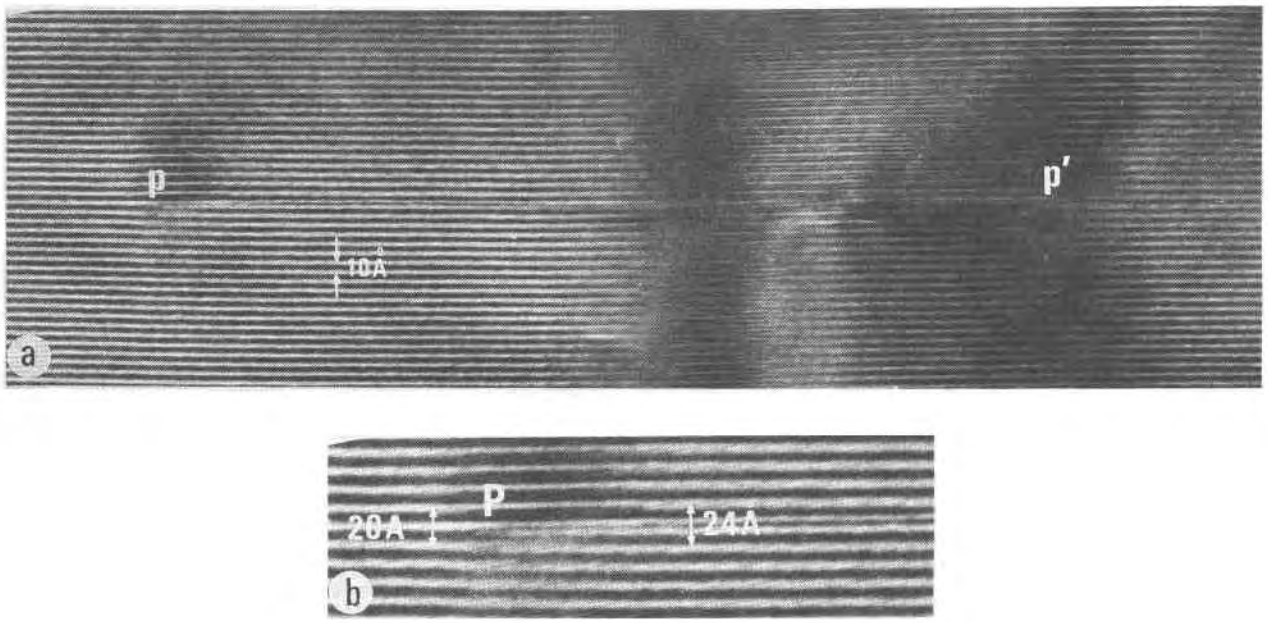

Fig. 3. Partial interlayering of a brucite-like sheet. a: the brucite layer extends between P and P'. b: enlargement of region P showing that the brucite layer is situated between two talc-like layers of the mica and terminates in the interlayer level.

white circle to a black one in Figure 1b. Due to the rearrangement of interlayer cations relative to the basal oxygens of T_1 and T_2, the interlayer sheet is expanded and the cohesion energy for this level is lowered (the lowering of this cohesion energy depends on the arrangement of interlayer cations and might reach 1 J/m^2 as a maximum value; see Olives and de Fouquet, 1982).

Brucite interlayering

Observation

HRTEM images show the presence of isolated partial layers interstratified in the mica structure (Fig. 3). Figure 3b shows that these layers are situated between two talc-like layers of the mica and terminate in the interlayer level. This pair of talc layers is limited by two interlayer levels, the distance between which increases from 20Å in the normal structure to 24±0.5Å (measured on several images) in the interstratified structure. It is most likely, therefore, that the extra layer is a brucite-like sheet, which forms, with one of the two adjacent talc-like sheets, a single chlorite layer. From a structural point of view, the interstratification is equivalent to the replacement of a plane of interlayer cations by a brucite-like sheet.

Intercalated brucite layers are easily damaged by ion and electron beam irradiation (during ion thinning of the specimen and during TEM observation). Figure 4 shows two brucite sheets strongly damaged, but a slight grey contrast is still present in the positions of the sheets. In Figure 5, no grey contrast occurs; the brucite layer has been completely destroyed. What remains unchanged in all cases is the distance of 24Å between the interlayer levels limiting the slab talc–brucite–talc.

Despite the destruction of the brucite sheet, Figure 5 provides precise information on the structure of the interlayer levels of the mica (see "Mica structure imaging"), which is in this case a biotite of 1M type. The shift between the spots of two interlayer levels separated by a talc-like layer is always zero. This absence of shift corresponds to layer staggers parallel to one another (1M stacking sequence) and perpendicular to the image plane (*i.e.*, perpendicular to [100]). Only the staggers of the two talc layers adjacent to the (destroyed) brucite sheet cannot be determined from the image Figure 5. Nevertheless, they are most likely identical to those of adjacent talc layers. Considering the spots situated on either side of the brucite sheet, the image shows that they are shifted relative to one another by 1.5Å. Thus, the two tetrahedral sheets adjacent to the brucite sheet are probably shifted by 1.5Å.

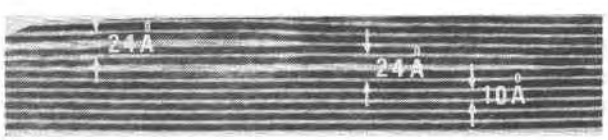

Fig. 4. Two interstratified brucite sheets in mica structure, damaged by ion and electron beam irradiation.

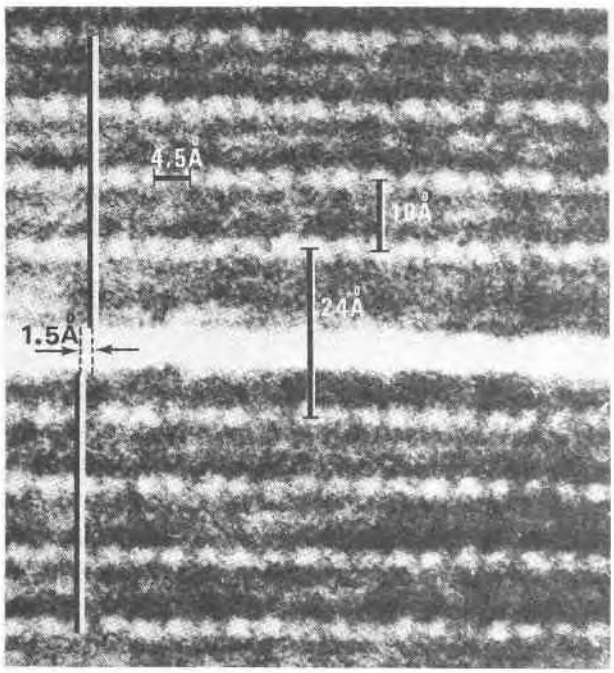

Fig. 5. Image of a 1M biotite viewed along [100] or [$\bar{1}$00]. "Channels" between the interlayer cations are imaged as bright spots of 4.5Å spacing. The interstratified brucite sheet has been completely destroyed by ion-electron beam irradiation. The upper interlayer levels are shifted toward the right relative to the lower ones by 1.5Å.

Stacking structure talc–brucite–talc

The intercalation structure of a brucite layer between two talc layers can be deduced from the chlorite structure, in which talc-like layers (T–O–T) and brucite-like layers (B) are alternately superimposed, with hydrogen ions between these layers. Each sheet, T, O, or B, is limited by two oxygen planes, and these may be numbered from 1 to 10 as follows:

(1)T(2)O(3)T(4)–(5)B(6)–(7)T(8)O(9)T(10).

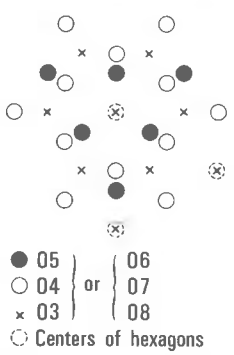

Fig. 6. Talc–brucite stacking structure: basal projection of the successive oxygen planes (see text).

The relative disposition of the oxygens O_3, O_4, and O_5 (or the equivalent O_8, O_7, and O_6) projected onto the basal plane is shown in Figure 6 (see Brown and Bailey, 1962). This figure shows that the oxygen plane O_5 (alternatively O_6) is shifted relative to O_3 (alternatively O_8) by a vector $\vec{x}$, which is equal to one third of one of the vectors joining two neighboring centers of the hexagons. As the brucite sheet is of octahedral structure, the two oxygen planes O_5 and O_6 are shifted by a vector of the same type as $\vec{x}$. Consequently, the shift between O_3 and O_8 ($\overrightarrow{O_3O_8} = \overrightarrow{O_3O_5} + \overrightarrow{O_5O_6} + \overrightarrow{O_6O_8}$) may be either $\vec{0}$ or a vector of the type $\vec{x}$. In Figure 1b, the O_3 oxygens are represented by black circles, and white circles when situated at the centers of the hexagons; the possible positions for O_8 oxygens are indicated by crosses (Fig. 1c). Let us denote respectively T_1 and T_2 the two tetrahedral sheets (3)T(4) and (7)T(8) adjacent to the brucite sheet. Then, the white circles in Figure 1c represent the centers of hexagons of T_1 and the crosses the possible positions for those of T_2 (since each O_8 oxygen may be a center of hexagon of T_2).

If the image plane is horizontal in Figure 1c, the apparent shift between two tetrahedral sheets separated by a brucite layer will be 0 or ±1.5Å. These apparent shifts are the same as those due to layer stagger (see "Mica structure imaging"). In the case of a brucite layer interstratified in the mica structure, the shift between the two interlayer levels limiting the slab talc–brucite–talc is the sum of three vectors: the staggers of the two talc layers and the shift between the two tetrahedral sheets adjacent to the brucite layer; each of these vectors has a projection onto the image plane of 0 or ±1.5Å. Therefore, the total apparent shift will be also 0 or ±1.5Å. The measured value of 1.5Å in Figure 5 is, in all cases, consistent with this structural interpretation.

Discussion

In Figure 5, the shift of 1.5Å probably involves the two tetrahedral sheets T_1 and T_2 adjacent to the brucite sheet. With reference to Figure 1c (with the image plane horizontal), the T_2 positions must belong to one of the two vertical rows of crosses distant by 1.5Å from the T_1 positions. Of all the possible positions, two particular ones (indicated by black circles in Fig. 1b) may be produced by partial slip between two tetrahedral sheets adjacent to an interlayer level.

Since the micas of the Bormes gneisses are deformed and the interstratified brucite-like layers are partial and isolated, we propose that the interlayering within these micas is derived from pre-existing deformation defects. We have shown that slip in micas occurs in the interlayer level, and that partial slip produces an expansion of the interlayer sheet and reduces the cohesion energy of this level. Consequently, diffusion within this level should be highly facilitated and a "brucitization" process (equivalent to a chloritization) may occur in the limited region of

the interlayer planar defect. Interlayer cations are substituted by a brucite-like sheet. Structurally, as noted above, this substitution requires no shift (except normal to the layers) between the two parts of the mica separated by the brucitization zone. Figure 1c shows that another process is structurally possible: brucitization after a cleavage. Indeed, after cleavage, the centers of T_2 hexagons coincide (on a basal projection) with those of T_1. Thus, in this position, a brucite sheet may be intercalated between T_1 and T_2 (crosses will then coincide with white circles).

We interpret the image in Figure 5 to represent brucitization after partial slip. More generally, we can conclude that brucitization after an interlayer partial slip or cleavage (via deformation processes) is a possible mechanism for brucite interlayering in micas.

Acknowledgments

We thank Georges Bronner, Claude Tempier and Michel Fonteilles who have provided the geological basis for this study.

References

Amouric, M., Baronnet, A. and Finck, C. (1978). Polytypisme et désordre dans les micas dioctaédriques synthétiques. Etude par imagerie de réseau. Material Research Bulletin, 13, 627–634.

Amouric, M., Mercuriot, G. and Baronnet, A. (1981) On computed and observed HRTEM images of perfect mica polytypes. Bulletin de Minéralogie, 104, 298–313.

Bell, I. A. and Wilson, C. J. L. (1977) Growth defects in metamorphic biotite. Physics and Chemistry of Minerals, 2, 153–169.

Bell, I. A. and Wilson, C. J.L. (1981). Deformation of biotite and muscovite: TEM microstructure and deformation model. Tectonophysics, 78, 201–228.

Brown, B. E. and Bailey, S. W. (1962). Chlorite polytypism: I. Regular and semi-random one-layer structures. American Mineralogist, 47, 819–850.

Caslavsky, J. L. and Vedam, K. (1970). The study of dislocations in muscovite mica by X-ray transmission topography. Philosophical Magazine, 22, 255–268.

Deville, J. P. and Goldsztaub, S. (1969). Etude du clivage de la muscovite par spectrométrie des électrons. Auger. Comptes Rendus de l'Académie des Sciences, Paris, B, 268, 629–630.

Iijima, S. and Buseck, P. R. (1978). Experimental study of disordered mica structure by HRTEM. Acta Crystallographica, A34, 709–719.

Iijima, S. and Zhu, J. (1982). Muscovite-biotite interface studied by electron microscopy. American Mineralogist, 67, 1195–1205.

McKee, T. R. and Buseck, P. R. (1978). HRTEM observation of stacking and ordered interstratification in rectorite. In J. M. Strugess, Ed., Electron Microscopy, 1, p. 272–273. Microscopical Society of Canada. Toronto.

Olives, J. and Fonteilles, M. (1980). Etude tectonique des terrains paléozoïques dans le Sud-Ouest du massif des Maures (Var, France). Revue de Géologie dynamique et de Géographie physique, Paris, 22, 123–134.

Olives, J. and de Fouquet, C. (1982). Energie de cohésion des défauts plans interfoliaires dans les micas. Comptes Rendus de l'Académie des Sciences, Paris, II, 294, 689–691.

Page, R. H. and Wenk, H. R. (1979). Phyllosilicate alteration of plagioclase studied by transmission electron microscopy. Geology, 7, 393–397.

Silk, E. C. H. and Barnes, R. S. (1961). The observation of dislocations in mica. Acta Metallurgica, 9, 558–562.

Sitarek, U. and Becherer, G. (1974). Interpretation of ribbon-like contrasts on X-ray topograms of muscovite monocrystals. Kristall und Technik, 9, 523–531.

Smith, J. V. and Yoder, H. S. (1956). Experimental and theoretical studies of the mica polymorphs. Mineralogical Magazine, 31, 209–235.

Tempier, C., Bronner, G., Gueirard, S. and Lécorché, J. P. (1980). Signification géologique des gneiss de Bormes. Chronologie des évènements dans le massif des Maures (Var). 8e Réunion Annuelle des Sciences de la Terre, Marseille, Société Géologique de France, p. 341.

Veblen, D. R. and Buseck, P. R. (1980). Microstructures and reaction mechanisms in biopyriboles. American Mineralogist, 65, 599–623.

Veblen, D. R. and Buseck, P. R. (1981). Hydrous pyriboles and sheet silicates in pyroxenes and uralites: intergrowth microstructures and reaction mechanisms. American Mineralogist, 66, 1107–1134.

Manuscript received, April 27, 1982;
accepted for publication, February 3, 1983.